NeuroImage 132 (2016) 491–498

Contents lists available at ScienceDirect

NeuroImage

journal homepage: www.elsevier.com/locate/ynimg

A cortical vascular model for examining the specificity of the laminar BOLD signal

Irati Markuerkiaga [a,*], Markus Barth [b], David G. Norris [a]

[a] Donders Centre for Cognitive Neuroimaging, Kapittelweg 29, 6542 EN Nijmegen, The Netherlands
[b] Centre for Advanced Imaging, The University of Queensland, Brisbane, Australia

ARTICLE INFO

Article history:
Received 11 August 2015
Accepted 26 February 2016
Available online 4 March 2016

Keywords:
Vascular cortical model
Layer specific BOLD fMRI
Spatial specificity
Gradient echo
Spin echo

ABSTRACT

Blood oxygenation level dependent (BOLD) functional MRI has been used for inferring layer specific activation in humans. However, intracortical veins perpendicular to the cortical surface are suspected to degrade the laminar specificity as they drain blood from the microvasculature and BOLD signal is carried over from lower to upper cortical layers on its way to the pial surface. In this work, a vascular model of the cortex is developed to investigate the laminar specificity of the BOLD signal for Spin Echo (SE) and Gradient Echo (GE) following the integrative model presented by Uludağ et al. (2009). The results of the simulation show that the laminar point spread function (PSF) of the BOLD signal presents similar features across all layers. The PSF for SE is highly localised whereas for GE there is a flat tail running to the pial surface, with amplitude less than a quarter of the response from the layer itself. Consequently the GE response at any layer will also contain a contribution accumulated from all lower layers.

Introduction

The human neocortex is a convoluted 2–3 mm thick neuronal sheet that is divided into six histological layers in most cortical areas. These layers have a generic pattern of feed-forward connections to higher order brain regions or feedback connections to lower order cortical or subcortical regions (Douglas and Martin, 2004; Thomson and Bannister, 2003). Layer specific functional activation patterns could hence improve the current understanding of within and between region connections at rest and activation.

Blood Oxygenation Level Dependent (BOLD) measurement by Magnetic Resonance Imaging (MRI) is the most commonly used non-invasive technique for measuring brain activation. The Spin Echo (SE) BOLD signal is generally considered to be less sensitive than the Gradient Echo (GE) BOLD signal, because the 180° refocusing pulse applied rephases the contributions in the static dephasing regime, i.e. the dephasing that results from the intravascular frequency offset (vascular dephasing) and the extravascular dephasing around vessels larger than 20 μm (Ogawa et al., 1993). However, if the intravascular dephasing contribution can be neglected because of a very short intravascular T2 -value, then the SE-BOLD signal is expected to be more spatially specific (Lee et al., 1999) because the remaining dynamic averaging contribution will be driven by smaller vessels that are closer to the site of neuronal activation (Boxerman et al., 1995). The GE-BOLD signal, on the contrary, will have a strong contribution from larger veins (Barth and Norris, 2007) and will therefore be more sensitive to changes in blood oxygenation but less spatially specific (Panchuelo et al., 2014).

These differences in the sensitivity of the BOLD signal between SE and GE sequences are particularly relevant for layer specific BOLD imaging. The cortical vasculature has a distinct arrangement by which a tangled microvascular network is drained by intracortical veins (ICV). These veins run perpendicular to the surface, drain blood along their way and flow into pial veins on the cortical surface (Duvernoy et al., 1981). Therefore, activation in a lower cortical layer will have an effect in upper layers as blood is carried through the cortex on its way to the pial surface. GE-BOLD data is expected to be more affected by this carry-over effect as it is more sensitive to larger vessels. To date, laminar BOLD measurements have been performed using both SE (Zhao et al., 2004; Harel et al., 2006; Goense and Logothetis, 2006) and GE (Polimeni et al., 2010; De Martino et al., 2013; Chen et al., 2013; Koopmans et al., 2009, 2011), yielding a range of BOLD profiles across the cortex for both types of MR sequences. The interpretation of these profiles remains problematic without some measure of the spatial point spread function for the BOLD response in differing experimental situations. Unlike conventional BOLD imaging which can utilise retinotopic mapping to obtain a measure of the spatial PSF (Engel et al., 1997) analogous experiments have not been established for laminar fMRI. Hence, modelling approaches remain as the sole possibility of better understanding the excitation profiles obtained experimentally.

In this paper a simple model of cortical vasculature is developed. The model is based on histological observations and captures the vascular differences across cortical layers in the human primary visual cortex (V1). Based on the local vascular features, the static BOLD response to

* Corresponding author.

http://dx.doi.org/10.1016/j.neuroimage.2016.02.073
1053-8119/

equal neurovascular response across the cortex is predicted following the two compartment BOLD signal model proposed by Uludağ et al. (2009). This model is then applied to analyse the laminar/ICV contributions to the total BOLD signal across the cortex; estimate the depth dependent laminar specificity of the BOLD signal and the laminar physiological point spread function (PSF) for both GE and SE.

Model and simulations

Vascular model of the cortex

In order to examine the laminar specificity of the BOLD signal, the cortical vasculature is divided into two parts in this work: 1) the intracortical veins (ICV) that run through the cortical layers perpendicular to the cortical surface, and 2) the part of the vasculature, which is composed of tangled, randomly oriented venules, capillaries and arterioles, called the *laminar network* here. The vascular model of the human primary visual cortex proposed is developed by combining the known volume and vessel distribution of the laminar network (Weber et al., 2008; Boas et al., 2008) with the density and features of ICVs (Duvernoy et al., 1981; Park et al., 2005b) in order to obtain the number and diameters of the ICVs required to drain the blood in the modelled cortical region. Arteries are not considered in this vascular model because it has been shown that their contribution to the BOLD signal at higher fields is negligible (Gagnon et al., 2015). For simplicity, pial veins are not part of this model, but their effect on the BOLD signal in the parenchyma will be discussed.

The laminar network

The vascular volume of the laminar network varies across the cortex between 2 and 2.7% and is on average 2.3% in the macaque V1 (Weber et al., 2008). The vascular compartment distribution of the laminar network in this model is 21% arterioles, 36% capillaries and 43% venules, which is derived from the Vascular Anatomical Network (VAN) proposed by Boas et al. (2008). This VAN is a vascular model that branches from one arteriole through 2^6 capillaries to one draining venule. In each of the six branching steps, a vessel splits into (arterial side) or reconnects (venous side) two vessels of a smaller diameter. Arterioles have a diameter between 10 and 30.5 μm, capillaries have a diameter of 8 μm and venules have a diameter between 12 and 36.6 μm. Between branching steps, all vessels are 100 μm long, except for the capillaries, which are 250 μm long.

Intracortical veins

Intracortical veins are perpendicular to the cortical surface and flow into large pial veins on the cortex. Duvernoy et al. (1981) provide a thorough description of ICVs and classify them in five groups based on their diameter and reach: V5 veins have an average diameter of 120 μm and emerge from white matter. Veins from groups V4, V3, V2 and V1 have average diameters of 60 μm, 45 μm, 30 μm and 20 μm, and originate in histological layers VI, IV, II/III and I, respectively. Intracortical veins drain all the layers they pass through and their diameters increase as they approach the surface because they are swollen by incoming laminar venules (Turner, 2002). The cortical layer boundaries of human V1 in the model were fixed following de Sousa et al. (2010) and Burkhalter and Bernardo (1989): layer VI, 20%; layer V, 10%; layer IV, 40%; layer II/III, 20%; layer I, 10% (values rounded to the closest multiple of 10). Hence, as the average cortical thickness of the primary visual cortex is 2.5 mm (Fischl and Dale, 2000), the thinnest cortical layers (layers V and I) are roughly 0.25 mm thick. In this work, the cortical vascular model comprises 10 voxels, with a base of 0.75×0.75 mm^2 and a height of 0.25 mm expanding from the WM/GM boundary to the cortical surface. Hence, the thinnest layers are one voxel thick and thicker layers extend over an integer number of voxels. However, the voxel size simulated is about three times smaller than the smallest voxel volumes used in experimental high resolution fMRI studies in humans. To allow a better comparison with experimentally obtained profiles, the BOLD signal across the cortex obtained using the 10 voxels is convolved with the smoothing kernel calculated in Koopmans et al. (2011). This kernel was calculated by projecting onto a line an isotropic voxel averaged over all possible orientations, to account for the blurring introduced by generating laminar profiles by integrating over extended patches of cortex, obtaining a FWHM of 87% of the voxel size.

Duvernoy et al. (1981) found that vessels are organised in a circular pattern on the cortical surface. Along the axis of each venous unit runs either one principal vein (ICV of group V5) or two intermediate size veins (ICVs of group V4 or V3). The diameter of a unit centred on intermediate size veins was 0.75–1 mm, whereas the diameter of those centred on a principal vein ranged from 1 to 4 mm. In line with the model voxel area given above, the vascular model developed is centred on two intermediate veins. This way, all model voxels belong to the same venous unit and partial voluming between adjacent venous units is avoided.

Regarding the intracortical vessel density across the cortex, MR-venography in the somatosensory cortex of rats and in the visual cortex of cats showed that ICV density increases roughly linearly from the lower part of the cortex (1 vein/mm^2) to the surface of the cortex (6 veins/mm^2) (Park et al., 2005a). These magnitudes do not vary much between the two species and brain regions considered, hence they are considered valid for human V1 too.

Once the characteristics of the ICVs are known, their diameters at each depth are calculated based on the laminar flow that needs to be drained, i.e. the total cross sectional capillary flow. Following (Zweifach and Lipowsky (1977) the velocity of blood through the vessels is roughly proportional to their diameter and therefore, as stated in Turner (2002), Murray's law applies, by which the sum of the cubes of the average radii of all capillaries in the layer and the radii in the entering layer boundary of the ICVs equals the sum of the cubes of the radii of the ICVs in the exiting layer boundary (Eq. (1)):

$$\sum_i r^3_{ICVout_i} = \sum_j r^3_{ICVin_j} + \sum_k r^3_{capLayer_k} \quad (1)$$

where i runs over the ICVs emerging from a layer, j over the ICVs entering that layer and k over the capillaries in the layer. The number of capillaries is obtained by dividing the capillary volume in a layer by the volume of one capillary. As the capillary volume across the cortex is known, iteratively applying Eq. (1) for each voxel starting from the voxel closest to the GM/WM boundary, the diameters of the ICVs across the cortex are obtained. It is assumed that laminar flow is equally distributed among the draining ICVs present in the voxel. The number of the V2 and V1 ICVs was chosen such that the number of ICVs increased roughly linearly and that the diameters obtained on the cortical surface were close to the observations in Duvernoy et al. (1981), as explained earlier.

Following the steps described here a vascular model is obtained in which the arteriole, capillary, venule and ICV volume density vary across the cortical depth. A schematic illustration of the main features of the vascular model is shown in Fig. 1. Based on these vascular features, the depth dependent BOLD signal can be predicted applying the BOLD signal model.

BOLD signal model

The static BOLD signal at rest is modelled as the volume weighted sum of the intravascular and extravascular BOLD signal (Eq. (2)), following Obata et al. (2004) and Uludağ et al. (2009):

$$S = (1-CBV)S_{EV} + \sum_i CBV_i S_{IV_i} \quad (2)$$

where CBV is the cerebrovascular volume, S_{EV} and S_{IV} are the BOLD signals arising from the extravascular and intravascular compartments,

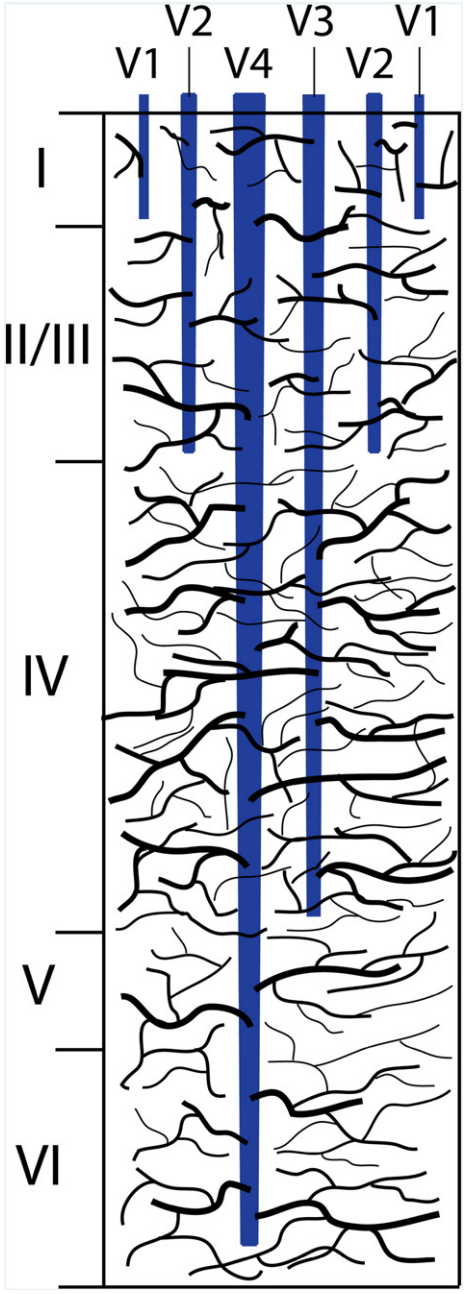

Fig. 1. Schematic representation of the vascular model developed. Intracortical veins (in blue) run perpendicular to the cortical surface and drain blood from all layers they pass through. The microvascular density is highest in layer IV.

respectively, and subindex i refers to the different vascular compartments (i.e. arterioles, capillaries, venules and intracortical veins). Activation of the cortical region leads to vascular dilation and changes in deoxyhaemoglobin content, altering the intravascular and extravascular signals and the vascular volume in the region. The fMRI signal, $\Delta BOLD = \Delta S/S_0$, is given as the normalised signal difference between the activation and baseline states.

If T1 relaxation can be neglected, the relaxation component of the MR signal can be described by a monoexponential function: $S_{EV,IV} = S_{0_{EV,IV}} e^{-(R2_{EV,IV}TE)}$. The parameters of the signal model in this simulation are set following Uludağ et al. (2009). As the BOLD signal change is normalised to its baseline value, S_0 can be considered to be equal to the proton densities of the extravascular and intravascular compartments, which, for simplicity, are considered to be equal in this work. The transversal relaxation rate $R_2^{(*)}$ can be given as the sum of the intrinsic, $R_{2,0}^{(*)}$, and deoxyhaemoglobin dependent, $R_{2,dHb}^{(*)}$, relaxation rates: $R_2^{(*)} = R_{2,0}^{(*)} + R_{2,dHb}^{(*)}$. Based on own or published in-vivo, ex-vivo and simulated data, Uludağ and colleagues provide a comprehensive compilation of intrinsic and oxygenation dependent relaxation rates for a range of field strengths between 1.5 and 16.1 T, blood oxygenation levels or vessel size and orientations both in the extravascular and intravascular compartments for SE and GE sequences (B_0: 1.5, 3, 4, 4.7. 7, 9.4, 11.7, 14 and 16.1 T and echo times for each simulated field of 96, 77, 65, 60, 50, 41, 33, 29 and 26 ms for SE and 66, 48, 41, 37, 28, 22, 19, 17 and 15 ms for GE).

The haemodynamic response to neural activation is modelled as an increase in the vascular volume and the blood oxygenation. Microvascular vessels, i.e. arterioles, capillaries and venules smaller than 20 μm in diameter, increase their volume by 16%, which under Grubb's law corresponds to a 50% increase in blood flow. Venules larger than 20 μm in the laminar network and ICVs are considered not to dilate as shown by Hillman et al. (2007). Regarding blood oxygenation, oxygen saturation, *Y*, increases from 60% to 70% in the postcapillary vessels, from 77.5% to 85% in the capillaries and from 95% to 100% in arterioles between the baseline and activated states.

The BOLD signal across the cortex is predicted on the basis of the number and diameters of the ICVs obtained from the vascular model and the known varying vascular density and distribution of the laminar network. The extravascular signal dephasing around the vessels depends, among other parameters, on their orientation with respect to B_0. Vessels in the laminar network can be considered to be randomly oriented, but intracortical vessels in a vascular unit are perpendicular to the surface and have a specific orientation. However, layer specific BOLD measurements in humans are generally processed by integrating the laminar BOLD signal along a convoluted patch of cortex. Along this integration line, the effect of ICVs can be considered to be that of randomly oriented, as their orientation with respect to B_0 will change with the curvature of the cortex. Thus, the results shown here are calculated by applying extravascular dephasing parameters calculated for randomly oriented vessels as given in Uludağ et al. (2009).

Analysis of the laminar BOLD signal

The vascular-BOLD model is implemented in MATLAB (2012a, The MathWorks, Inc.) and predicts the equilibrium BOLD response across the cortex to a continuous stimulus. These simulations assume equal net excitatory neuronal activity and neurovascular coupling across the cortex. Similarly, it is considered that the haemodynamic response spatially overlaps with the underlying neural activity and that it is laminar specific as suggested by the combination of depth dependent electrophysiological and BOLD signal onset time measurements to whisker pad stimulation in rats (Jones et al., 2004 and Yu et al., 2014, respectively).

This work analyses the BOLD signal contributions of the laminar vasculature and ICVs in order to examine the laminar BOLD specificity and the carry over or signal leakage to more superficial layers. This unidirectional leakage (i.e. from the layer of activation towards the cortical surface) is obtained by calculating the downstream changes in oxygenation and blood flow for each layer. The Point Spread Function (PSF) of the BOLD signal is then calculated for each layer. These curves do not represent the activation of a point but rather of a small volume of activated cortex, i.e. the small voxel of $0.75 \times 0.75 \times 0.25$ mm^3 used in the simulations, which is considered to be sufficiently small to analyse the variation of the PSF between layers.

The peak to tail ratio, is defined as the ratio between the magnitude of the peak of the laminar PSF and the average magnitude of the tail over all downstream layers. Lastly, in order to illustrate how the underlying neurovascular response affects the physiological PSF, the peak to tail ratio is explored under different strengths of regional haemodynamic and metabolic responses for 3 T and 7 T. The regional blood flow–metabolism coupling constant n ($n = \%\Delta CBF/\%\Delta CMRO_2$), ΔCBF and

$\Delta CMRO_2$ percentage changes upon activation for a visual stimulus of a flickering checkerboard with 10% and 40% contrasts and a movie were obtained from Griffeth et al. (2014). It is assumed that the haemodynamic response scales equally in all layers with these reported regional variations and the oxygen saturation Y in the vasculature is obtained applying Fick's principle (Kim et al., 1999).

Given that high (sub-millimetre) resolution fMRI benefits especially from the increase in MR sensitivity at 7 T (Triantafyllou et al., 2005) and following recent laminar fMRI studies (Polimeni et al., 2010; Koopmans et al., 2011; Olman et al., 2012; Siero et al., 2013), laminar specificity comparisons between SE and GE are given at this field strength for simplicity. The features of the physiological point spread function are given for a range of field strengths between 1.5 T and 16 T to assess the variation of the laminar specificity across fields.

Results

Intracortical veins and vascular volume

The diameters of the intracortical veins obtained are in line with the average values reported by Duvernoy et al. (1981), as shown in Table 1. These results reflect the fact that the vascular territory drained by a single vessel has a cone-like shape, with its broad base in the lower layers. V4, for example, drains a larger territory in layer V, where it is the only type of vein present, than in layer II/III, which is drained by several types of ICVs. According to Lorthois et al. (2011), the vascular territory drained by a vessel of 55 μm diameter will have a radius of 340 μm, which corresponds to the vascular territory drained by V4 in layers V and VI in the model developed here.

The calculated vascular volume across the cortex of the laminar and ICVs (Fig. 2) is in good agreement with the measurements related to the depth-dependent vascular density performed by Cassot et al. (2006) using confocal laser microscopy in excised and ink-injected sections of human cortex. The contribution of the laminar network to the total vascular volume is larger all across the cortical depth, even though ICV volume increases roughly from 0.2% to 1.5% as the cortical surface is approached.

BOLD response across the cortex

The intravascular and extravascular contributions to the BOLD signal changes are shown in Fig. 3(a,b). For the SE-BOLD response the EV contribution is almost twice as strong as the IV contribution and the BOLD profile has a maximum where the laminar vascular density is highest, which corresponds to histological layer IV. For GE, under the working assumption made in this paper following Uludağ et al. (2009), the IV contribution to the BOLD signal is neglected from 7 T upwards and hence the BOLD signal is entirely of extravascular origin. Note that pial vessels are not considered in this model, therefore the cortical GE-BOLD profile shown is the result of the decrease in vascular density from the cortical surface to the GM/WM boundary (Fig. 2), especially due to the decrease in ICV density, and is not related to the long ranging effects of pial vessels at the cortical surface. Table 2 shows that the magnitude of the simulated BOLD responses is within the experimental ranges obtained in awake humans at 7 T.

Table 1
Average vessel diameters (in μm) of the intracortical veins across the cortex of a vascular unit centred around two smaller vessels of groups V4 and V3. The vascular unit has one vein of groups V4 and V3 and two veins of groups V2 and V1.

	V4	V3	2 × V2	2 × V1
Layer VI	41.4			
Layer V	52.4			
Layer IV	59.1	39.1		
Layer II/III	63.6	48.4	24.6	
Layer I	64.6	50.1	30.2	19.0

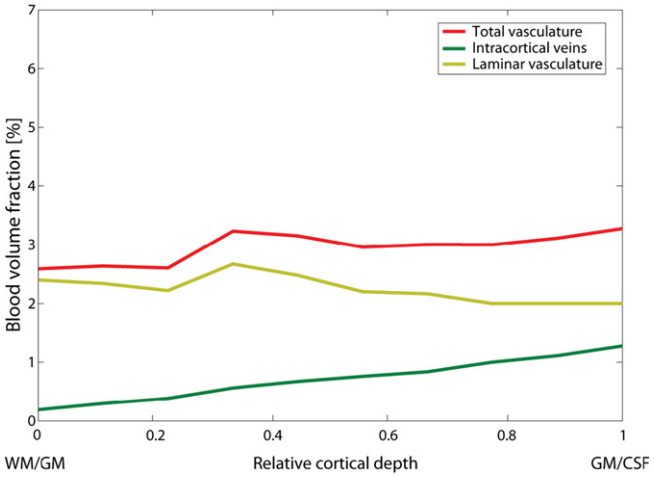

Fig. 2. CBV volume fraction across the modelled cortex for the laminar network (yellow), intracortical veins (green) and the sum of the ICV and laminar network vascular volume (red).

As expected, the SE-BOLD signal is highly laminar specific as it is dominated by the laminar contribution at all cortical depths, Fig. 3(c,e). The GE-BOLD signal, on the other hand, is driven by ICVs for the most part of the cortex, especially in upper cortical layers, where the ICV density is also highest Fig. 3(d). In this sense, it is apparent from Fig. 3(e,f) that the laminar specificity of the BOLD signal decreases as the cortical surface is approached, most significantly for GE-BOLD. Under the current simulation parameters of equal metabolic and vascular response across the cortex, most of the GE-BOLD signal obtained in the upper layers is the result of activation in lower cortical layers.

The laminar PSF of the BOLD signal for different layers are shown in Fig. 4(a) and (b), for SE and GE respectively. The laminar PSF for layer I is not given as ICVs here drain into pial veins on the cortex. These curves present two interesting features: first, the laminar spread function shows very little variation between layers, neither for SE nor for GE. As shown in Fig. 3, the SE-BOLD data has very little contribution from ICVs, hence the SE-BOLD signal is highly laminar specific and spreads very little through the cortex (Fig. 4(a)). GE-BOLD data, on the contrary, has a considerable contribution from ICVs, and hence a larger laminar spread, but this does not vary much between layers either. Second, the tail of the BOLD signal spread is rather constant through the layers downstream of the activation site. This occurs despite the fact that blood oxygenation in ICVs decreases as they approach the cortical surface and blood drained from the activated layer is diluted with blood from non-activated layers. The explanation for this apparently counter-intuitive phenomenon is that the diameters of the ICVs increase with decreasing cortical depth. The extravascular signal decay around randomly oriented vessels between 16 and 200 μm varies in a near linear fashion with both the oxygen saturation and the volume of the vessel (Uludağ et al., 2009). This means that the expected decrease in BOLD signal difference due to the dilution effect is compensated by the increased volume of the vessels, and hence the tail of the BOLD signal spread remains nearly constant.

The ratio between the peak and the average magnitude of the tail is defined as the peak to tail ratio. Fig. 5(a) shows the field strength dependence of this ratio for GE-BOLD data. The trend for SE-BOLD is not shown because it is high enough to be considered laminar specific across all field strengths (the lowest value is obtained for 3 T and it is over 30). The average across lamina of the peak to tail ratio is between 4 and 7 for field strengths between 1.5 T and 16 T. It has a minimum at 7 T, the field strength at which our working hypothesis assumes that the IV contribution vanishes, and from here on it increases steadily with increasing B0. In the presence of an IV contribution of 10% to the

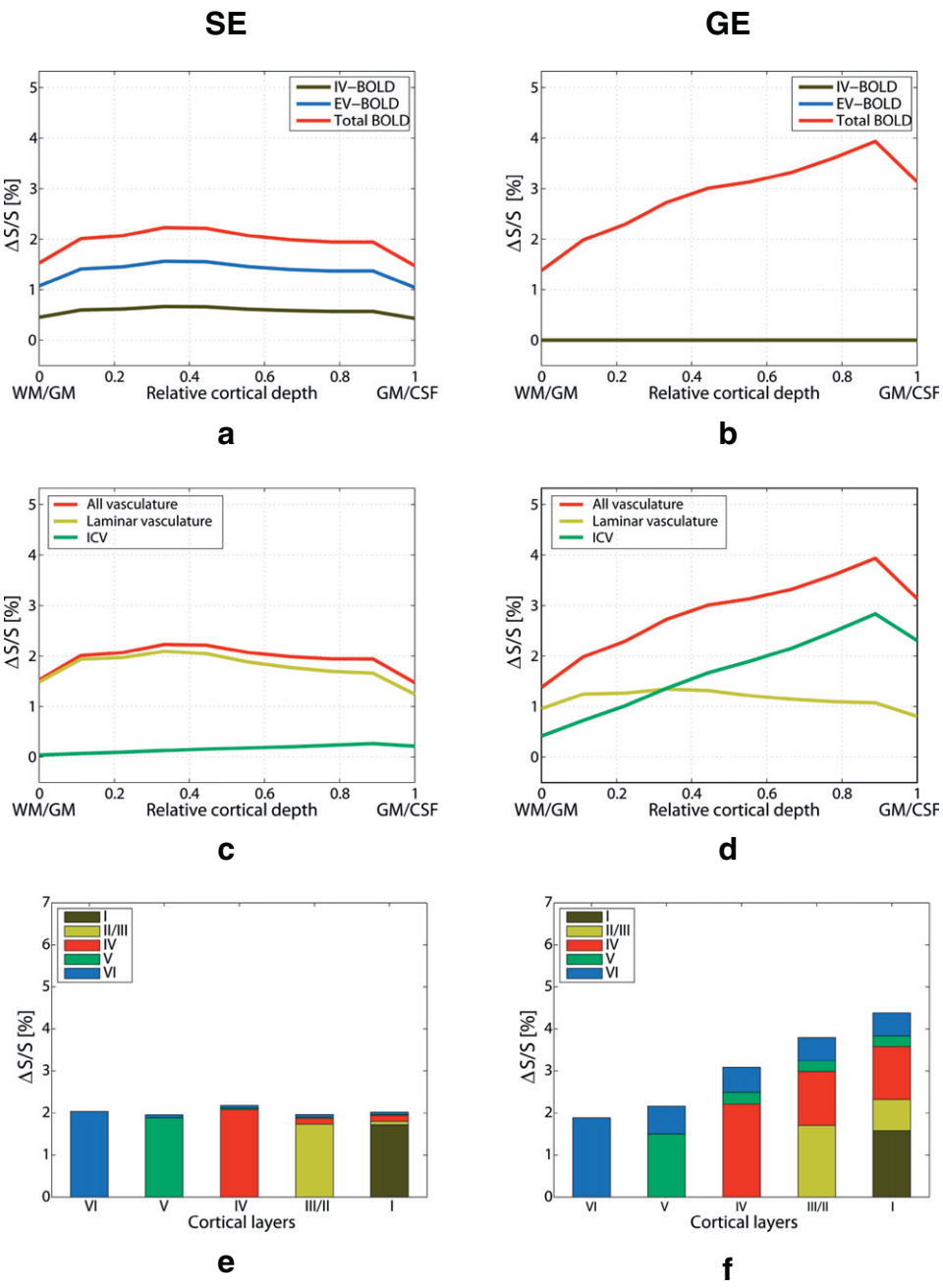

Fig. 3. First row: total (red), intravascular (brown) and extravascular (blue) activation profiles across the cortex. Second row: laminar network (yellow), ICV (green) and total (red) activation profiles along the cortex. Third row: the BOLD signal broken down according to the contribution from the same layer and layers upstream. Note that all simulation were using $B_0 = 7$ T, $TE_{SE} = 50$ ms, and $TE_{GE} = 28$ ms and that the thickness and the total vascular volume of the layers are not equal. The left column refers to SE and the right column to GE.

Table 2
Quantitative comparison of simulated profiles with experimental values reported in the literature for 7 T in awake humans. The ranges in the table refer to minimum and maximum magnitude of the BOLD signal profile across the cortex. Experimental values were obtained in the visual[a,b,d,e,f] and motor[c] cortices ([a]Polimeni et al. (2010); [b]Koopmans et al. (2011); [c]Huber et al. (2015); [d]De Martino et al. (2013); [e]Siero et al. (2015); [f]Kemper et al. (2015)).

	Simulation (manuscript)	Experimental studies (literature)
Spin echo	1.5–2.3%	1–2%[f]
Gradient echo	1.5–4%	2–4%[a,c,d]
		0.5–3%[b]
		1.5–5%[e]

total BOLD signal at 7 T, for example, this ratio will be higher and the minimum will be shifted to lower field strengths. However, the curve is useful to give a notion of upper and lower bounds of laminar specificity across field strengths for GE-BOLD data. Further, in this work, the BOLD profiles after integrating over an extended convoluted patch of cortex are simulated, and hence ICVs are considered to be randomly oriented. However, if no such extended integration is performed, the peak to tail ratio will vary with the orientation of the cortex. For example, if ICVs are oriented perpendicularly to B_0, their contribution to the BOLD signal increases, and compared to the simulated peak to tail ratios at 7 T shown in this work, the peak to tail ratio will be reduced by about 25% (data not shown).

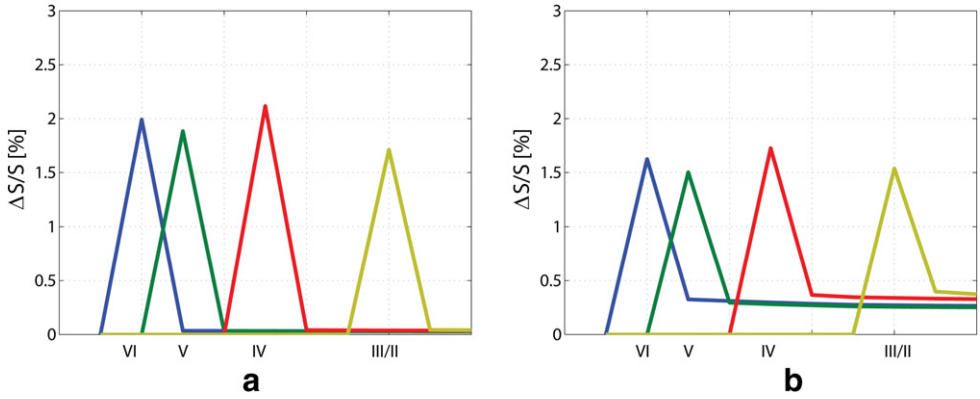

Fig. 4. The laminar BOLD PSF at 7 T for the activation of a $0.75 \times 0.75 \times 0.25$ mm^3 voxel within a single layer located in layer VI (blue), V (green), IV (red) and II/III (yellow) for SE (a) and GE (b).

The results shown in Fig. 5(b) suggest that peak to tail variations based on changes of CBF follow a similar pattern across field strengths (results shown for 3 T and 7 T) and that the peak to tail ratio or the laminar specificity is comparable for low contrast visual stimuli.

Discussion

A vascular model of the primary visual cortex has been developed to examine the laminar specificity of the BOLD signal. The activation profiles through the cortex obtained in Fig. 3(a,b) are similar to those obtained by Goense and Logothetis (2006), Polimeni et al. (2010), De Martino et al. (2013), Zhao et al. (2004) and Chen et al. (2013). As expected, the results of the simulation show that there is BOLD signal leakage from lower layers to upper layers through the intracortical veins (Fig. 3(d,f)).

Laminar specificity of SE- and GE-BOLD signal

Fig. 3(e,f) show that SE-BOLD signal is highly layer specific whereas the laminar specificity of GE-BOLD signal decreases as the cortical surface is approached. In fact, for equal vascular and metabolic responses across all layers, the cumulative contribution from lower layers is higher than the laminar GE-BOLD signal in superficial layers. This carry-over effect implies that care must be taken when comparing activation strengths between the different lamina within a region, or inferring connectivity between more distant regions when GE sequences are used. The use of differential designs (i.e. subtracting BOLD signal layer profiles for tasks with different layer distributions), as in Trampel et al. (2012), Olman et al. (2012) and Panchuelo et al. (2014), can alleviate the carry over effect considerably (see Supplementary Information).

The laminar PSF in Fig. 4 shows some interesting features: the peak to tail ratio does not vary considerably between layers and the tail remains rather constant across the downstream layers. In addition, the peak to tail ratios are comparable for similar CBF–CMRO2 coupling constants and varying CBF increase upon activation (Fig. 5(b)). These properties of the laminar PSF could form the basis for a deconvolution or forward model fitting approach that would facilitate the extraction of the laminar specific BOLD signal for GE-BOLD. It is interesting to note the laminar BOLD signal change is stronger for SE than GE sequences at the commonly used echo times of 50 ms and 28 ms, respectively, (see laminar BOLD signal contributions (in blue) in Fig. 3(c,d)). However, SE sequences are RF intensive, which results in a higher power deposition that, at the high field strengths and resolutions favoured for laminar fMRI, might hit SAR limits. Further, it is difficult to collect high resolution SE data over extended volumes of cortex with a reasonable TR and the lengthy read-out required, especially for SE-EPI, introduces a non-negligible T2' contribution (Goense and Logothetis, 2006).

Neurovascular response across the cortex

In the simulation results presented here, the vascular response is assumed to be equal across the cortex. However, the vascular response is expected to vary with cortical depth as neuronal activity is not expected to be evenly distributed over the cortical layers. It has been shown that in response to visual stimulation, neural circuits within layer IV tend to

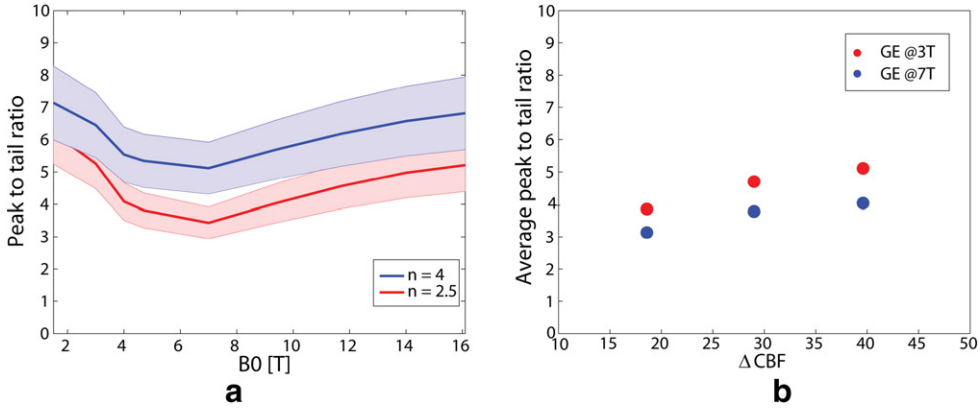

Fig. 5. (a) The average laminar peak to tail ratio across field strengths for GE-BOLD (the shaded region represents the standard deviation) for $n = 4$ (red), as in Uludağ et al. (2009), and $n = 2.5$ (blue), average n in Griffeth et al. (2014). (b) The average peak to tail ratio for GE-BOLD at 3 T (red) and 7 T (blue) for the regional CBF increases and blood flow–metabolism coupling constant n reported in Griffeth et al. (2014) ($n = 2.5 \pm 0.2$).

consume more energy compared to other layers, reflecting laminar differences in glucose uptake (Tootell et al., 1988), and that there are long-term changes in neuronal activity related to metabolic activity (Horton, 1984). The BOLD signal reflects the input and intracortical processing in a region more, as measured by the local field potential (LFP) (Logothetis et al., 2001). Hence, cortical depth dependent electrophysiological recordings of LFP obtained with array probes could potentially be used as a measure of the underlying neural activity that drives the BOLD response.

Intravascular T2 and signal relaxation during read-out

The parameters of the BOLD signal model have all been taken from the comprehensive article by Uludağ et al. (2009) and, following this work, the intravascular contribution to the GE-BOLD signal at 7 T (and above) has been neglected. However, Donahue et al. (2011) showed that in fMRI measurements using 3.5 mm isotropic voxels at 7 T, the EV-BOLD contribution to the total GE-BOLD signal was between 75 and 90%. Cortical GE-BOLD signal profiles and PSF with an intravascular contribution at 7 T of 10% and 23% are shown in SI1. The specificity of the laminar activation, which is measured as the peak to tail ratio in this work, increases with increasing intravascular contribution because the volume of laminar vasculature is higher than the volume of ICVs all across the cortex (Fig. 2) and the higher SO_2 change in the ICV compared to arterioles and capillaries does not compensate for the differences in volume. Nonetheless, the BOLD profiles and shape of the PSF are similar with and without the presence of an intravascular contribution to the BOLD signal and its presence does not considerably change the conclusions of this work.

Further, T2' weighting as a result of signal relaxation during readout in non purely SE sequences such as SE-EPI, has been neglected. Hence, the results here represent the highest attainable laminar specificity. As experimentally shown by Goense and Logothetis (2006) and Budde et al. (2014), the longer the acquisition window used the larger the contribution from larger veins is in SE-BOLD data, because of the increase in the T2' weighting of the acquired signal.

Validity of the simulations with regard to the duration of the stimulus

In this work, veins larger than 20 μm were assumed not to dilate, but it is worth discussing the stimulus condition that applies to this physiological response. There are a number of publications that investigated venous dilation with regard to the length of the stimuli used. It has been reported that venous dilation is negligible for stimuli shorter than 20 s (Hillman et al., 2007; Kim et al., 2007; Kim and Kim, 2011), whereas for stimuli longer than 20 s venous dilation was observed (Drew et al., 2011; Huo et al., 2015; Kim and Kim, 2011).

In this manuscript the static BOLD response to activation was simulated. As the transit time through the cortical vasculature (i.e. from pial arteries back to pial veins) is around 1 s, for stimuli longer than this duration there will be a period in the delayed BOLD response (~6 s after the onset of the stimulus) in which the cortex will be in the steady state in which our simulation conditions hold. Therefore, the simulation conditions apply for stimuli in the range from 1 s to 20 s.

Effect of pial veins in the parenchyma

On average, one vein between 0.1–1 mm drains each side of the occipital lobe (Andrews et al., 1989), but most of the central veins have a diameter between 280 and 380 μm and peripheral veins of 130 μm (Duvernoy et al., 1981). Given the low number of 1 mm diameter veins, the strongest possible long ranging effect of a 380 μm pial vein was studied to assess the long ranging effects of pial vessels on the parenchyma (data not shown). In this situation the vessel has to be oriented perpendicularly to B_0, a lobe of the dipolar field has to be perpendicular to the cortical surface, and the pial vessel experiences the maximum oxygenation change upon activation considered in this model, which will occur as a consequence of the full activation of a circular cortical area 9.7 mm in diameter. Even when using this worst case scenario, the field dephasing induced across the first 250 μm from pial surface into the parenchyma (i.e. first simulated voxel) is only roughly a quarter of the intravoxel dephasing induced by the laminar network in this layer. As the long ranging effect decays with $1/r^2$, in the next 250 μm the dephasing is already negligible. Smaller pial veins can induce a stronger dephasing along the first 250 μm, but will be negligible for the rest of the cortical profile. Therefore, in the absence of partial volume effects, the long range effect is confined to the superficial layer I. For a plausible voxel size for laminar BOLD signal, such as a 0.75 mm isotropic voxel and due to the convoluted cortex (effect of the pial veins will be randomised), integration would reduce these effects further.

Validity of the vascular model

The laminar vascular density across the cortex in this model follows the vascular density in macaque V1 reported by Weber et al. (2008). This distribution is in agreement with other works that report an increased vascular density in layer IV (Duvernoy et al., 1981; Zheng et al., 1991) and roughly corresponds to the description of vascular layers in Lauwers et al. (2008), in which authors show a profile that is slightly flatter and smaller in microvascular density for the human collateral sulcus. The microvascular distribution of venules, capillaries, and arterioles obtained following the VAN model proposed by Boas et al. (2008) is in line with Weber et al. (2008) in macaque V1.

The region modelled is the primary visual cortex of primates because there is extensive literature on histological and functional studies that focus in this region. By considering the regional vascular density, cortical thickness and layer distribution, similar models can be analogously developed for other brain areas. The combined vascular-BOLD model is deterministic and easy to implement. In this work, the static BOLD response is simulated, which makes the model simpler and computationally less demanding. However, as presented here, the model is not applicable to event-related measurements in which the temporal dynamics of blood flow along its draining path have to be considered.

Other approaches to obtain laminar BOLD

A number of approaches for obtaining laminar BOLD signal for GE acquisitions that do not involve the use of a vascular model have been reported. In Fracasso et al. (2014) the cortical GE-BOLD profile is separated into a strong linear component, which is assumed to be related to larger veins, and a weak linear component, which is believed to be related to the microvasculature in the laminar network. In Chen et al. (2013) the top 40% most activated voxels are removed, as they are considered to be venous voxels, and the laminar GE-BOLD signal is obtained considering only the remaining voxels. Lastly, Yu et al. (2012) show direct contributions of microvasculature and macrovasculature to the BOLD signal by measuring at high temporal and spatial resolution in a reduced FOV to investigate feed-forward and feed-back connections in rats.

Conclusion

This paper describes a model of cortical vasculature that is used to predict the static BOLD response across the cortex following the signal model as proposed by Uludağ et al. (2009). The model separates the contribution to the BOLD signal of different vascular compartments to investigate laminar specificity. The simulation predicts that, under equal neurovascular response across the cortex, SE-BOLD signal is highly laminar specific, whereas GE-BOLD signal is less specific as activation in a layer is carried over to layers downstream through intracortical veins. The laminar specificity of the GE-BOLD signal decreases with increasing ICV volume as the cortical surface is approached. The features

of the laminar point spread functions, however, are rather similar across layers and could potentially be used in a forward model or deconvolution to extract the laminar BOLD signals free of BOLD signal leakage from layers upstream.

Acknowledgments

We thank Dr. Jan van der Eerden for critical comments on this manuscript. Preliminary results of this work have been presented in the 22nd Annual Meetings of ISMRM, Milan, Italy, p. 3093. This work was funded by the Initial Training Network in High resolution Magnetic Resonance (HiMR) within the FP7 Marie Curie Actions of the European Commission (FP7-PEOPLE-2012-ITN-316716). MB acknowledges funding from the ARC Future Fellowship grant FT140100865.

Appendix A. Supplementary data

Supplementary data to this article can be found online at http://dx.doi.org/10.1016/j.neuroimage.2016.02.073.

References

Andrews, B.T., et al., 1989. Microsurgical Anatomy of the Venous Drainage into the Superior Sagittal Sinus.
Barth, M., Norris, D.G., 2007. Very high-resolution three-dimensional functional MRI of the human visual cortex with elimination of large venous vessels. NMR Biomed. 20, 477–484.
Boas, D.A., et al., 2008. A vascular anatomical network model of the spatio-temporal response to brain activation. NeuroImage 40 (3), 1116–1129.
Boxerman, J.L., et al., 1995. MR contrast due to intravascular magnetic-susceptibility perturbations. Magn. Reson. Med. 34, 555–566.
Budde, J., et al., 2014. Functional MRI in human subjects with gradient-echo and spin-echo EPI at 9.4 T. Magn. Reson. Med. 71 (1), 209–218.
Burkhalter, A., Bernardo, K.L., 1989. Organization of Corticocortical Connections in Human Visual Cortex 86 pp. 1071–1075 (February).
Cassot, F., et al., 2006. A novel three-dimensional computer-assisted method for a quantitative study of microvascular networks of the human cerebral cortex. Microcirculation (New York, N.Y.: 1994) 13 (1), 1–18.
Chen, G., et al., 2013. Layer-specific BOLD activation in awake monkey V1 revealed by ultra-high spatial resolution functional magnetic resonance imaging. NeuroImage 64, 147–155.
DE Martino, F., et al., 2013. Cortical depth dependent functional responses in humans at 7 T: improved specificity with 3D GRASE. PLoS One 8 (3), e60514.
DE Sousa, A.A., et al., 2010. Comparative cytoarchitectural analyses of striate and extrastriate areas in hominoids. Cerebral Cortex (New York, N.Y.: 1991) 20 (4), 966–981.
Donahue, M.J., et al., 2011. Blood oxygenation level-dependent (BOLD) total and extravascular signal changes and $\Delta R2^*$ in human visual cortex at 1.5, 3.0 and 7.0 T. NMR Biomed. 24 (1), 25–34.
Douglas, R.J., Martin, K.A.C., 2004. Neuronal circuits of the neocortex. Annu. Rev. Neurosci. 27, 419–451.
Drew, P.J., Shih, A.Y., Kleinfeld, D., 2011. Fluctuating and sensory-induced vasodynamics in rodent cortex extend arteriole capacity. Proc. Natl. Acad. Sci. 108 (20), 8473–8478.
Duvernoy, H.M., Delon, S., Vannson, J.L., 1981. Cortical blood vessels of the human brain. Brain Res. Bull. 7 (5), 519–579.
Engel, S.A., Glover, G.H., Wandell, B.A., 1997. Retinotopic organization in human visual cortex and the spatial precision of functional MRI. Cereb. Cortex 7 (2), 181–192.
Fischl, B., Dale, A.M., 2000. Measuring the Thickness of the Human Cerebral Cortex from Magnetic Resonance Images (Track II).
Fracasso, A., Petridou, N., Dumoulin, S.O., 2014. Distinct BOLD laminar profiles elicited by retino-cortical and inter-hemispheric sources in human early visual cortex. Proc. Int. Soc. Magn. Reson. Med. 52 (5), 4435.
Gagnon, L., et al., 2015. Quantifying the microvascular origin of BOLD-fMRI from first principles with two-photon microscopy and an oxygen-sensitive nanoprobe. J. Neurosci. 35 (8), 3663–3675.
Goense, J.B.M., Logothetis, N.K., 2006. Laminar specificity in monkey V1 using high-resolution SE-fMRI. Magn. Reson. Imaging 24 (4), 381–392.
Griffeth, V.E.M., Simon, A.B., Buxton, R.B., 2014. The coupling of cerebral blood flow and oxygen metabolism with brain activation is similar for simple and complex stimuli in human primary visual cortex. NeuroImage 104, 156–162.
Harel, N., et al., 2006. Combined imaging-histological study of cortical laminar specificity of fMRI signals. NeuroImage 29 (3), 879–887.
Hillman, E.M.C., et al., 2007. Depth-resolved optical imaging and microscopy of vascular compartment dynamics during somatosensory stimulation. NeuroImage 35 (1), 89–104.
Horton, J.C., 1984. Cytochrome oxidase patches: a new cytoarchitectonic feature of monkey visual cortex. *Philos. Trans. R. Soc. Lond. Ser. B Biol. Sci.* 304 (1119), 199–253.
Huber, L., et al., 2015. Cortical lamina-dependent blood volume changes in human brain at 7 T. NeuroImage 107, 23–33.
Huo, B.-X., Gao, Y.-R., Drew, P.J., 2015. Quantitative separation of arterial and venous cerebral blood volume increases during voluntary locomotion. NeuroImage 105, 369–379.
Jones, M., et al., 2004. Nonlinear coupling of neural activity and CBF in rodent barrel cortex. NeuroImage 22, 956–965.
Kemper, V.G., et al., 2015. Sub-millimeter T2 weighted fMRI at 7 T: comparison of 3D-GRASE and 2D SE-EPI. Front. Neurosci. 9, 163 (May).
Kim, S., et al., 1999. Determination of relative CMRO 2 from CBF and BOLD changes : significant increase of oxygen consumption rate during visual stimulation. Magn. Reson. Med. 1161 (41), 1152–1161.
Kim, T., et al., 2007. Arterial versus total blood volume changes during neural activity-induced cerebral blood flow change: implication for BOLD fMRI. J. Cereb. Blood Flow Metab. 27 (6), 1235–1247.
Kim, T., Kim, S.-G., 2011. Temporal dynamics and spatial specificity of arterial and venous blood volume changes during visual stimulation: implication for BOLD quantification. J. Cereb. Blood Flow Metab. 31 (5), 1211–1222.
Koopmans, P.J., et al., 2009. Distinguishing pial and laminar gradient-echo BOLD signals at 7 Tesla. Proc. Int. Soc. Magn. Reson. Med. 2009, 4064.
Koopmans, P.J., et al., 2011. Multi-echo fMRI of the cortical laminae in humans at 7 T. NeuroImage 56 (3), 1276–1285.
Lauwers, F., et al., 2008. Morphometry of the human cerebral cortex microcirculation: general characteristics and space-related profiles. NeuroImage 39 (3), 936–948.
Lee, S.P., et al., 1999. Diffusion-weighted spin-echo fMRI at 9.4 T: microvascular/tissue contribution to BOLD signal changes. Magn. Reson. Med. 42 (5), 919–928.
Logothetis, N.K., et al., 2001. Neurophysiological investigation of the basis of the fMRI signal. Nature 412 (6843), 150–157.
Lorthois, S., Cassot, F., Lauwers, F., 2011. Simulation study of brain blood flow regulation by intra-cortical arterioles in an anatomically accurate large human vascular network: part I: methodology and baseline flow. NeuroImage 54 (2), 1031–1042.
Obata, T., et al., 2004. Discrepancies between BOLD and flow dynamics in primary and supplementary motor areas: application of the balloon model to the interpretation of BOLD transients. NeuroImage 21 (1), 144–153.
Ogawa, S., et al., 1993. Functional brain mapping by blood oxygenation level-dependent contrast magnetic resonance imaging. A comparison of signal characteristics with a biophysical model. Biophys. J. 64 (3), 803–812.
Olman, C.A., et al., 2012. Layer-specific fMRI reflects different neuronal computations at different depths in human V1. PLoS One 7 (3), e32536.
Panchuelo, R.M.S., et al., 2014. Assessing the spatial precision of SE and GE-BOLD contrast at 7 Tesla. Brain Topogr. 62–65.
Park, J.C., et al., 2005b. Spatial Specificity of High Resolution Gradient Echo (GE) BOLD and Spin Echo (SE) BOLD fMRI in Cat Visual Cortex at 9. 4 13(2004) p. 67530.
Park, S., Hayashi, T., Kim, S., 2005a. Determination of Intracortical Venous Vessel Density Using Venography at 9.4 T 13(c) p. 15203.
Polimeni, J.R., et al., 2010. Laminar analysis of 7 T BOLD using an imposed spatial activation pattern in human V1. NeuroImage 52 (4), 1334–1346.
Siero, J.C.W., et al., 2013. BOLD specificity and dynamics evaluated in humans at 7 T: comparing gradient-echo and spin-echo hemodynamic responses. PLoS One 8 (1), e54560.
Siero, J.C.W., et al., 2015. Cortical depth dependence of the BOLD initial dip and poststimulus undershoot in human visual cortex at 7 Tesla. Magn. Reson. Med. 73 (6), 2283–2295.
Thomson, A.M., Bannister, A.P., 2003. Interlaminar connections in the neocortex. Cerebral Cortex (New York, N.Y.: 1991) 13 (1), 5–14.
Tootell, R., et al., 1988. Functional anatomy of macaque striate cortex. I. Ocular dominance, binocular interactions, and baseline conditions. J. Neurosci. 8 (5), 1500–1530.
Trampel, R., et al., 2012. Laminar-specific fingerprints of different sensorimotor areas obtained during imagined and actual finger tapping. Proc. Int. Soc. Magn. Reson. Med. 20, 663.
Triantafyllou, C., et al., 2005. Comparison of physiological noise at 1.5 T, 3 T and 7 T and optimization of fMRI acquisition parameters. NeuroImage 26 (1), 243–250.
Turner, R., 2002. How much cortex can a vein drain? Downstream dilution of activation-related cerebral blood oxygenation changes. NeuroImage 16 (4), 1062–1067.
Uludağ, K., Müller-Bierl, B., Uğurbil, K., 2009. An integrative model for neuronal activity-induced signal changes for gradient and spin echo functional imaging. NeuroImage 48 (1), 150–165.
Weber, B., et al., 2008. The microvascular system of the striate and extrastriate visual cortex of the macaque. Cerebral Cortex (New York, N.Y.: 1991) 18 (10), 2318–2330.
Yu, X., et al., 2012. Direct imaging of macrovascular and microvascular contributions to BOLD fMRI in layers IV–V of the rat whisker-barrel cortex. NeuroImage 59 (2), 1451–1460.
Yu, X., et al., 2014. Deciphering laminar-specific neural inputs with line-scanning fMRI. Nat. Methods 11 (1), 55–58.
Zhao, F., Wang, P., Kim, S.-G., 2004. Cortical depth-dependent gradient-echo and spin-echo BOLD fMRI at 9.4 T. Magn. Reson. Med./Soc. Magn. Reson. Med. 51 (3), 518–524.
Zheng, D., LaMantia, A.-S., Purves, D., 1991. Specialized vascularization of the primate visual cortex. J. Neurosci. 2622–2629 (August).
Zweifach, B.W., Lipowsky, H.H., 1977. Quantitative studies of microcirculatory structure and function. III. Microvascular hemodynamics of cat mesentery and rabbit omentum. Circ. Res. 41 (3), 380–390.